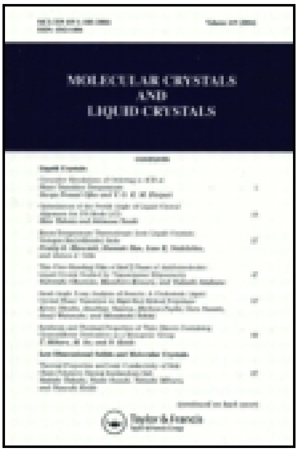

Molecular Crystals and Liquid Crystals
Publication details, including instructions for authors and subscription information:
http://www.tandfonline.com/loi/gmcl20

Synthesis and Properties of Hybrid Poly(3-Methylthiophene)-CdSe Nanocomposite and Estimation of Its Photovoltaic Ability

N. A. Ogurtsov [a], A. A. Pud [a], O. P. Dimitriev [b], Yu. P. Piryatinski [c], P. S. Smertenko [b], Yu. V. Noskov [a] & A. S. Kutsenko [d]

[a] Institute of Bioorganic Chemistry and Petrochemistry of NASU, Kyiv, Ukraine

[b] Institute of Semiconductor Physics of NASU, Kyiv, Ukraine

[c] Institute of Physics of NASU, Kyiv, Ukraine

[d] Institute of Physical Chemistry of NASU, Kyiv, Ukraine

Version of record first published: 03 Mar 2011

To cite this article: N. A. Ogurtsov, A. A. Pud, O. P. Dimitriev, Yu. P. Piryatinski, P. S. Smertenko, Yu. V. Noskov & A. S. Kutsenko (2011): Synthesis and Properties of Hybrid Poly(3-Methylthiophene)-CdSe Nanocomposite and Estimation of Its Photovoltaic Ability, Molecular Crystals and Liquid Crystals, 536:1, 33/[265]-40/[272]

To link to this article: http://dx.doi.org/10.1080/15421406.2011.538330

Mol. Cryst. Liq. Cryst., Vol. 536: pp. 33/[265]–40/[272], 2011
Copyright © Taylor & Francis Group, LLC
ISSN: 1542-1406 print/1563-5287 online
DOI: 10.1080/15421406.2011.538330

Taylor & Francis
Taylor & Francis Group

Synthesis and Properties of Hybrid Poly(3-Methylthiophene)-CdSe Nanocomposite and Estimation of Its Photovoltaic Ability

N. A. OGURTSOV,[1] A. A. PUD,[1] O. P. DIMITRIEV,[2]
YU. P. PIRYATINSKI,[3] P. S. SMERTENKO,[2]
YU. V. NOSKOV,[1] AND A. S. KUTSENKO[4]

[1]Institute of Bioorganic Chemistry and Petrochemistry of NASU, Kyiv, Ukraine
[2]Institute of Semiconductor Physics of NASU, Kyiv, Ukraine
[3]Institute of Physics of NASU, Kyiv, Ukraine
[4]Institute of Physical Chemistry of NASU, Kyiv, Ukraine

We report the synthesis and properties of new hybrid nanocomposites of poly (3-methylthiophene) and CdSe nanoparticles. The synthesis method is based on the chemical oxidative polymerization of 3-methylthiophene in the presence of CdSe nanoparticles of different shapes (quantum dots, nanorods, and tetrapods). In situ, *the open circuit potential and the UV-Vis monitoring of a reaction mixture are used to control the polymerization process. The minimal and maximal CdSe concentrations in nanocomposites are obtained for quantum dots and nanorods, respectively. Nanocomposites are investigated, by using IR, electronic absorption, and photoluminescence spectroscopies, TGA, and DTA. Hybrid photovoltaic (PV) cells based on these materials are fabricated and evaluated. The best PV performance is achieved for a device based on nanocomposites with CdSe nanorods.*

Keywords Bulk heterojunction cell; CdSe nanoparticles; poly(3-methylthiophene)

1. Introduction

Hybrid nanocomposites in the form of bulk heterojunction (BHJ) structures of conductive polymers and inorganic semiconductor nanocrystals have attracted a great attention in photovoltaics due to a possibility of the mutually complementary light absorption of components, as well as a possibility of the charge separation at their interface. In case of the realization of the transport of fast electrons and holes by interpenetrating inorganic and polymer networks formed inside a nanocomposite and the effective charge collection at electrodes, these materials will have real competitive applications in a cheap segment of PV devices. An easy synthetic possibility to change the hybrid nanocomposite properties by tuning both size and shape

---

Address correspondence to N. A. Ogurtsov, Institute of Bioorganic Chemistry and Petrochemistry of NASU, 50, Kharkivske Sh., Kyiv 02160, Ukraine. E-mail: nogurtsov@yahoo.com

of nanoparticles and a structure of conducting polymers is very important for the improvement of characteristics of these devices and for the achievement of cost-effective solar energy converters.

Among materials used in these systems, a great attention is drawn to polyalkylthiophenes in combination with CdSe [1–7]. There are several approaches to prepare such composites. One of the important methods is the preparation of a joint solution of CdSe nanoparticles and the conjugated polymer poly-3(hexylthiophene) (P3HT). Specifically, the PV device based on CdSe nanorods and P3HT showed a power conversion efficiency up to 1.7% under A.M. 1.5 Global solar conditions [2]. Using 1,2,4-trichlorobenzene as a high boiling temperature solvent for P3HT allowed one to obtain a fibrillar morphology which provides extended pathways for the hole transport. Blend devices fabricated with the use of this solvent gave solar power conversion efficiencies of 2.6% [3]. To control the interface structure and the blend morphology, a specially designed chemical interaction between the components was proposed [4]. To this end, phosphonic-acid-functionalized oligothiophenes have been synthesized and bound to the nanocrystal surface. The molecular composites of P3HT containing a diaminopyrimidine side group with 1-(6-mercaptohexyl)thymine capped CdSe nanocrystals via hydrogen bonds were designed [5,6]. Nanocomposites of P3HT-CdSe were synthesized by the direct grafting of vinyl-terminated P3HT onto [(4-bromophenyl)methyl]dioctylphosphine oxide functionalized CdSe quantum dot surfaces [7].

However, the above approaches are still based on the use of expensive P3HT. At the same time, quite efficient planar *p-n* type and Schottky-type heterojunctions based on a cheaper polymer, i.e., poly (3-methylthiophene) (P3MT), and CdSe were obtained. CdSe layers were deposited by the chemical bath deposition and P3MT was synthesized by the electrochemical method. The energy conversion efficiency of these junctions for a nonoptimized PV was 0.03 and 1.3%, respectively [8]. When CdSe was modified by silicotungstic acid, the energy conversion efficiency increased up to 2.7% for the Schottky-type photovoltaic P3MT-CdSe junction [8]. Thin film Zener diodes from P3MT and CdSe nanoparticles have been prepared by self-assembling trioctylphosphine oxide capped CdSe nanoparticles and 1,6-hexadecanethiol onto a chemically deposited P3MT layer [9]. The comparison of these P3MT-based planar devices with the above P3HT-based BHJ devices suggests that it is desirable to apply P3MT in the BHJ structure to develop a cheaper effective device. Obviously, the main problem here is the insolubility of this polymer.

To bypass this problem, we propose here an alternative approach which allows covering the inorganic nanoparticles with a shell of P3MT. This core-shell structure can have an improved interaction between its components and, as a consequence, can facilitate the charge separation at the donor-acceptor interface. To estimate the applicability of this approach, we have synthesized and characterized a series of new organic/inorganic hybrid nanocomposites of CdSe nanoparticles and P3MT.

2. Experimental

3-Methylthiophene (Merck), a 1.3 wt.% water dispersion of poly(3,4-ethylenedioxythiophene)-poly(styrenesulfonate) (PEDOT:PSS) (Aldrich), poly(3-hexylthiophene) (Rieke Metals), and other chemicals were used as-received.

CdSe quantum dots (CdSe-qd; the size was ~4–5 nm according to transmission electron microscopy (TEM) images) have been synthesized by water route [10], by using 1-thioglicerine as a stabilizer. Syntheses of CdSe tetrapods (CdSe-tp; the arm ~3 × 6 nm according to TEM images) and nanorods (CdSe-nr; the size ~4 × 30 nm according to TEM images) by the organometallic route were performed in accord with methods described in [11] and [12], by applying oleic acid and trioctylphoshine oxide as stabilizers, respectively, followed by their removal by the repetitive boiling with pyridine.

The hybrid materials were prepared through the chemical oxidative polymerization of 3-methylthiophene (3MT) by anhydrous $FeCl_3$ in acetonitrile in the presence of CdSe nanoparticles, at the constant weight ratio of 3MT:CdSe = 1:2 for all samples, in argon in a temperature-controlled (18°C) one-compartment cell upon stirring. The polymerization process was monitored *in situ* by continuously measuring the open circuit potential (OCP) of a Pt electrode *versus* the Ag/AgCl saturated reference electrode immersed in a reaction mixture. A digital pH/mV/Thermometer GMH3530 (Graisinger Electron., Germany) was used to record OCP curves. The reference sample of the individual P3MT was synthesized under similar conditions. The polymerization course was also periodically monitored by the survey of UV-Vis spectra in quartz cuvettes ($l = 1$ mm) of samples taken from the reaction mixture.

After the polymerization has been completed, P3MT and its nanocomposites were separated by the centrifugation and carefully washed with acetonitrile and methanol until the disappearance of the $FeCl_3$ bands in the UV-Vis spectra of washing liquors. The obtained P3MT was then dedoped by a surplus of hydrazine (50-% water solution) followed by washing with methanol and drying.

UV-Vis and IR spectra were recorded using spectrophotometers Cary 50 (Varian) and Specord M-80 (Karl Ceiss). Thermogravimetry analyses (TGA) and differential thermal analyses (DTA) of the samples were performed in air with a Derivatograph system F. Paulik, J. Paulik, L. Erdey with a heating rate 10°C/min in air using platinum crucibles. TEM images were obtained with a JEOL JEM-100CXII microscope. PL of the sample was excited by the 337-nm nitrogen laser radiation and measured using a home-made setup [13].

Model samples of hybrid solar cells were fabricated as a structure of ITO/PEDOT:PSS/active BHJ layer/Al. Before the cell preparations, ITO substrates were successively washed by the ultrasonication in acetone and then in 2-propanol pure water followed by the oxidative treatment with boiling H_2O_2 and dried in air. These substrates were then spin-coated by a PEDOT-PSS layer from its above-mentioned dispersion at 2000 rpm for 20 s followed by baking at 120°C for 30 min in argon. These PEDOT:PSS coated substrates were spin-coated with active CdSe-P3MT nanocomposite BHJ layers from their 1 wt.% dispersions in chlorobenzene at 2000 rpm for 20 s. Then they were again baked at 120°C for 30 min in argon. Aluminum was thermally evaporated as a top electrode. Current-voltage characteristics were measured in dark and under illumination using a halogen lamp with a power radiation being equivalent to 0.03 sun. Quasi-dc measurements were performed by a standard automated tester 14 TKS-100 (Russia). The voltage sweep was applied to the heterostructure step-by-step with the duration of each step being 250 ms and the measurement time being 90 ms.

3. Results and Discussion

Using the molar ratio 3MT:$FeCl_3$ = 1:2.7 typical of the alkylthiophene polymerization [14–16], we have found that the 3MT polymerization does not proceed in the

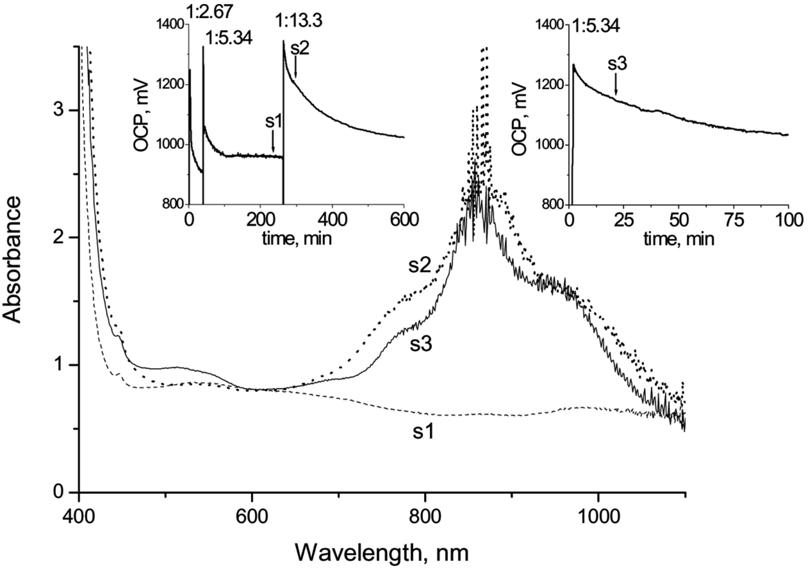

Figure 1. OCP profiles (insets) of the polymerization mixtures which are monitored at variable molar ratios 3MT:$FeCl_3$, and UV-Vis spectra of samples s1–3. Upper-left inset: $C_{3MT} = 0.01\,M$, $C_{CdSe\text{-}nr} = 2.08\,mg/ml$; upper-right inset: $C_{3MT} = 0.016\,M$, $C_{CdSe\text{-}nr} = 3.33\,mg/ml$. Arrows indicate the time when samples were taken from the reaction mixture.

presence of CdSe nanoparticles. The analysis of the OCP profile of the polymerization mixture of 3MT:CdSe nanoparticles after the addition of a necessary quantity of oxidant $FeCl_3$ (Fig. 1, upper-right insert, given here by the example of CdSe-nr, which is typical also of CdSe-qd and CdSe-tp) suggested that the oxidation potential in the system was not enough to ensure the polymerization process. Indeed, its middle value was ~0.8–1 V instead of the known necessary value to be not less than 1.1 V for the acetonitrile medium [17].

The addition of a second portion of $FeCl_3$ also did not result in OCP values being enough for the 3MT polymerization and the appearance of characteristic bands of doped P3MT in the near-IR region around 860 nm as well (Fig. 1, see the OCP profile in the upper-left inset, and the UV-Vis spectrum of the sample s1). But the necessary OCP values have been reached, and the P3MT bands appeared after a further increase of the 3MT:$FeCl_3$ molar ratio in favor of $FeCl_3$ till 1:13.3 (Fig. 1, see the OCP profile in the upper-left inset and the UV-Vis spectrum of the sample s2). On the other hand, we could realize the 3MT polymerization at higher monomer concentrations ($\geq$15 mM) in the presence of CdSe nanoparticles even at the lower ratio 1:5.34 (Fig. 1, see the OCP profile in the upper-right inset and the UV-Vis spectrum of the sample s3).

The observed 3MT polymerization behavior in the presence of CdSe nanoparticles allowed us to assume that the oxidation potential suppression and the existence of the minimal concentration of 3MT could be caused by the side reaction of CdSe oxidation by $FeCl_3$. This side process resulted in the consumption of the oxidant and a partial dissolution of CdSe. This assumption was confirmed by both a decrease of OCP of $FeCl_3$ solution in the presence of only CdSe nanoparticles and DTA curves of the synthesized P3MT-CdSe nanocomposites, which contained the endothermic peak of the elemental Se melting at ~216°C (not shown).

The presence of P3MT in the synthesized composites was confirmed by their IR and UV-Vis spectra (not shown) containing a set of bands corresponding to P3MT. Specifically, IR spectra contain the band at 1444 cm^{-1} which may be assigned to $C_\alpha{=}C_\beta$ symmetric stretching vibrations in thienilene rings and the band at 825 cm^{-1} due to the C–H out-of-plane deformation which are characteristic of 2,3,5-trisubstituted thiophene. The spectra contain also the bands at 1297 cm^{-1} and 1154 cm^{-1} which are characteristic of P3MT.

The presence of P3MT in the CdSe-P3MT nanocomposites is displayed also in their UV-Vis spectra (not shown) with a wide band at ~406 nm which corresponds to the π-π^* transition of conjugated alkylthiophene units [18]. On the other hand, this band masks the absorption of CdSe nanoparticles which are present in the nanocomposites.

Using TGA and DTA data, we determined an approximate composition of the nanocomposites (Table 1). Specifically, the complete burning of the nanocomposite in air gave the CdO residue which could appear due to the oxidation of CdSe. Therefore, the CdSe content was calculated from the solid residue. The contribution from the organic part of the nanocomposite, i.e., P3MT, was found as a difference between the initial weight of the analyzed sample and the calculated CdSe weight, respectively. The Se content was estimated from DTA curves of nanocomposites and Se powder.

As can be seen from Table 1, the compositions of the nanocomposites differ significantly, depending on the type of nanoparticles used. The minimal CdSe concentration was obtained for the CdSe-qd-P3MT nanocomposite (12 wt.%), and the maximal one was obtained for the CdSe-nr-P3MT nanocomposite (53 wt.%). This indicates that the dissolution rates of various types of CdSe nanoparticles are different. Obviously, this is related to distinctions in the sizes of used particles, which results in the their different surface areas. Indeed, despite the same initial weight loading, the smallest nanoparticles (CdSe-qd) have a maximal interphase contact area with the polymerization environment and the maximal reaction activity, respectively. A possibility to vary the CdSe content in the nanocomposites due to a change of the size of initial particles and the weight ratio of 3MT:CdSe will be studied later on.

The PL spectrum of the hybrid nanocomposite showed a broad emission band with the maximum at ~560 nm (Fig. 2, curve 3) and indicated a contribution of both P3MT and CdSe (see Fig. 2, curves 1, 2), being not a simple superposition of their emission. Specifically, an intermediate position of the nanocomposite PL band, which is close by position and similar by shape to the P3MT one, testifies to not only some specific interactions along the interface P3MT/CdSe but obviously to a less

Table 1. Approximate composition of nanocomposites and nanoparticles

Sample	CdSe, wt. %	P3MT, wt. %	Se, wt. %
CdSe-qd-P3MT	12	64	24
CdSe-nr-P3MT	53	47	Trace quantity
CdSe-tp-P3MT	28	61	11

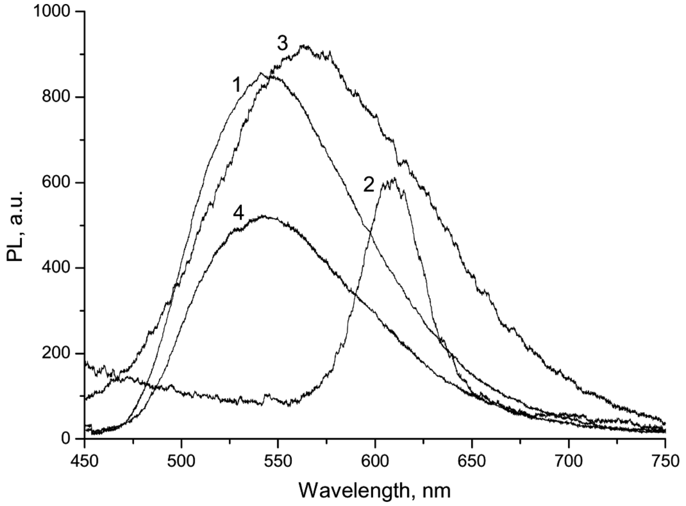

Figure 2. PL spectra of (1) a soluble fraction of P3MT in chlorobenzene (0.2 mg/ml), (2) CdSe-nr dispersion in acetonitrile (0.5 mg/ml), (3) the composite P3MT-CdSe dispersion in acetonitrile (0.5 mg/ml), and (4) PL emission of a P3MT solution in chlorobenzene (0.2 mg/ml) upon the addition of the CdSe dispersion (weight ratio 1:2%).

contribution of CdSe nanoparticles. The latter is confirmed by the above DTA data on the presence of Se in the nanocomposite. On the other hand, the possibility of the interactions is justified by the quite efficient quenching of PL of the P3MT by added CdSe nanoparticles (Fig. 2, curves 1,2 and 4). In turn, this quenching indicates also that the polymer-to-nanoparticle energy or a charge transfer process occurs at their interface.

In order to find the contribution of charge transfer processes, the photovoltaic performance of devices based on BHJs of CdSe-P3MT has been studied. The PV properties of ITO/PEDOT:PSS/nanocomposites/Al cells based on these materials are characterized by measuring the current–voltage dependences in dark and at 10 mW cm^{-2} of white light illumination through the ITO side (Fig. 3, curves 1–3). The best performance of the PV device was obtained when the CdSe-nr-P3MT BHJ was used. Specifically, the ITO/PEDOT:PSS/CdSe-nr-P3MT/Al heterostructure showed a much greater photocurrent than other heterostructures. This result well agrees with a low content of CdSe-qd and a middle content of CdSe-tp in the nanocomposites (Table 1) which are much lower than the content being critical to get the percolation threshold of the BHJ [1]. At the same time, the photovoltage (V_{oc}) was the highest in case of the ITO/PEDOT:PSS/CdSe-tp-P3MT/Al heterostructure. An increase of V_{oc} for CdSe-tp-P3MT has been observed probably due to the influence of a morphology of nanoparticles.

A significant improvement of the PV performance was observed for the BHJ active layer of the ternary nanocomposite based on a mixture of P3HT and CdSe-nr-P3MT nanocomposite (Fig. 3, curve 5) as compared both with that of the CdSe-nr-P3MT nanocomposite (Fig. 3, curve 3) and a mixture of CdSe nanorods with P3HT (Fig. 3, curve 4). Such an improvement can be related to the percolation change of the network of clusters in the BHJ layer. However, this effect requires a further study.

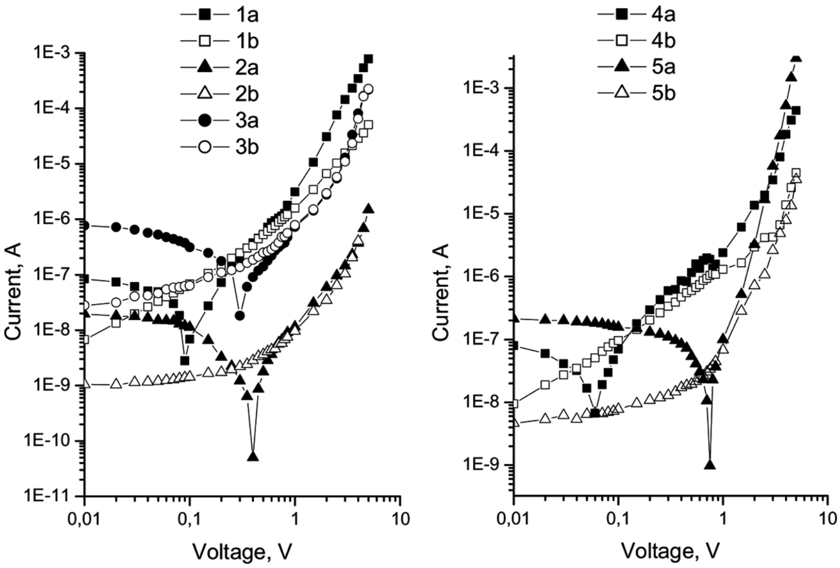

Figure 3. Current-voltage characteristics of ITO/PEDOT:PSS/nanocomposite/Al cells: (a) under white light and (b) in dark, where BHJ active layers of nanocomposites are: (1) – CdSe-qd-P3MT synthesized nanocomposite, (2) – CdSe-tp-P3MT synthesized nanocomposite, (3) – CdSe-nr-P3MT synthesized nanocomposite, (4) – mechanical mixture of CdSe-nr and P3HT (80:20 wt.%), and (5) – mixture of CdSe-nr-P3MT synthesized nanocomposite and P3HT (80:20 wt.%).

4. Conclusion

A facile method to synthesize nanocomposites of CdSe and poly(3-methylthiophene) with pronounced PV properties has been developed. It has been found that the polymerization process is decelerated by CdSe nanoparticles unlike the known polymerization processes in the presence of the dispersion phase. Specifically, the 3MT polymerization can be realized with a registered rate only at molar ratios of 3MT:$FeCl_3$ favoring the increased concentration of oxidant $FeCl_3$ being significantly higher than that suitable for the synthesis of individual P3MT. The parallel OCP and UV-Vis methods are very useful tools for tracking and controlling the nanocomposite synthesis. It has been found that CdSe nanoparticles can effectively quench the PL emission of P3MT.

The prepared ITO/PEDOT:PSS/CdSe-nr-P3MT/Al heterostructure showed a much greater photocurrent than that in heterostructures based on nanocomposites of CdSe-tp and CdSe-qd, but V_{oc} had the highest value in the case of the CdSe-tp nanocomposite.

The obtained results demonstrated a possibility of the formation of a solar cell based on the active BHJ layer made of polymer/inorganic hybrid nanocomposites containing nanoparticles with shells of the insoluble photoactive polymer (P3MT) and the inorganic semiconductor core of CdSe nanoparticles.

Acknowledgment

The financial support of STCU project No. 3746 is gratefully acknowledged.

References

[1] Saunders, B. R., & Turner, M. L. (2008). *Adv. Colloid Interface Sci.*, *138*, 1.

[2] Huynh, W. U., Dittmer, J. J., & Alivisatos, A. P. (2002). *Science*, *295*, 2425.

[3] Sun, B., & Greenham, N. C. (2006). *Phys. Chem. Chem. Phys.*, *8*, 3557.

[4] Milliron, D. J., Alivisatos, A. P., Pitois, C., Edder, C., & Frechet, J. M. J. (2003). *Adv. Mater.*, *15*, 58.

[5] De Girolamo, J., Reiss, P., & Pron, A. (2007). *J. Phys. Chem. C*, *111*, 14681.

[6] De Girolamo, J., Reiss, P., Zagorska, M., De Bettignies, R., Bailly, S., Mevellec, J.-Y., Lefrant, S., Travers, J.-P., & Pron, A. (2008). *Phys. Chem. Chem. Phys.*, *10*, 4027.

[7] Xu, J., Wang, J., Mitchell, M., Mukherjee, P., Jeffries-EL, M., Petrich, J. W., & Lin, Z. (2007). *J. Am. Chem. Soc.*, *129*, 12828.

[8] Sène, C., Nguyen Cong, H., Dieng, M., & Chartier, P. (2000). *Mat. Res. Bull.*, *35*, 1541.

[9] Cassagneau, T., Mallouk, T. E., & Fendler, J. H. (1998). *J. Am. Chem. Soc.*, *120*, 7848.

[10] Raevskaya, A. E., Stroyuk, A. L., Kuchmiy, S. Ya., Azhniuk, Yu. M., Dzhagan, V. M., Yukhymchuk, V. O., & Valakh, M. Ya. (2006). *Colloid Surface A*, *290*, 304.

[11] Pang, Q., Zhao, L., Cai, Y., Nguyen, D. P., Regnault, N., Wang, N., Yang, S., Ge, W., Ferreira, R., Bastard, G., & Wang, J. (2005). *Chem. Mater.*, *17*, 5263.

[12] Gur, I., Fromer, N. A., Geier, M. L., & Alivisatos, A. P. (2005). *Science*, *310*, 462.

[13] Piryatinski, Yu. P., & Yaroshchuk, O. V. (2000). *Opt. Spectrosc.*, *89*, 860.

[14] Sugimoto, R., Takeda, S., Gu, H. B., & Yoshino, K. (1986). *Chem. Express*, *1*, 635.

[15] Leclerc, M., Diaz, F. M., & Wegner, G. (1989). *Makromol. Chem.*, *190*, 3105.

[16] McCullough, R. D. (1998). *Adv. Mater.*, *10*, 93.

[17] Zotti, G., Zecchin, S., Schiavon, G., Vercelli, B., & Berlin, A. (2005). *J. Electroanal. Chem.*, *575*, 169.

[18] Patil, A. O., Heeger, A. J., & Wudl, F. (1988). *Chem. Rev.*, *88*, 183.